Chinese Chemical Letters 34 (2023) 108411

Contents lists available at ScienceDirect

Chinese Chemical Letters

journal homepage: www.elsevier.com/locate/cclet

Dye@MOF composites (RhB@**1**): Highly sensitive dual emission sensor for the detection of pesticides, Fe^{3+} and ascorbate acid

Lu Liu, Xiao-Li Chen*, Miao Cai, Rui-Kui Yan, Hua-Li Cui, Hua Yang, Ji-Jiang Wang

School of Chemistry and Chemical Engineering, Shaanxi Key Laboratory of Chemical Reaction Engineering, Laboratory of New Energy and New Function Materials, Yan'an University, Yan'an 716000, China

ARTICLE INFO

Article history:
Received 1 November 2022
Revised 11 February 2023
Accepted 30 March 2023
Available online 31 March 2023

Keywords:
Metal-organic framework
Rhodamine B
Pesticides
Fe^{3+}
Ascorbate acid
Fluorescence sensing

ABSTRACT

With the rapid development of economy, industrial and agricultural pollutants have caused great damage to the ecological environment and the normal development of organisms, posing a serious threat to global public health. Therefore, rapid and sensitive detection of pollutants is very important for environmental safety and people's health. A stable multi-response fluorescence sensor (RhB@**1**) with dual emission characteristics was constructed by embedding RhB guest molecules in Zn-MOF using a simple one-pot method. XRD, IR, XPS, Raman and other characterization methods were used to demonstrate the formation of composite materials. The sensor has two fluorescence emission peaks at 415 nm and 575 nm under the excitation of 316 nm. It has high sensitivity and low detection limit (7.94 and 7.82 nmol/L, respectively) in the detection of fluazinam (FLU) and Fe^{3+}. The mechanism of fluorescence quenching may be due to the synergistic effect of IFE and PET. Outstandingly, when ascorbate acid (AA) was added to the quenching system of Fe^{3+} and RhB@**1**, its fluorescence gradually recovered, forming the unique "on-off-on" sensor. Therefore, RhB@**1** has a fast fluorescence response and good stability, making it potentially useful in practical application and biosensors. More significantly, using Fe^{3+} and AA as chemical input signals, a binary intelligent logic gate device has been developed based on the "on-off-on" response mode of RhB@**1**, which extends the application of logic gate switching devices in the chemical field. In addition, a visual portable test paper with good selectivity and high sensitivity was developed, which can be used for rapid detection of FLU, showing its broad application prospect.

At present, the research of luminesent materials is one of the host spots in the field of chemistry, especially quantum dots, perovskites and metal-organic framework (MOF) [1–3]. MOFs, have attracted great attention in the field of luminescence sensing [4–8], dye degradation [9,10], catalysis [11] and biomedicine [12,13] due to their diverse structure and adjustable size of micropores. However, many structurally stable MOF properties are too simple, which greatly limits its application. Therefore, many researchers try to explore ways to expand its application without affecting its structural integrity. By means of adsorption, ion exchange, post-synthetic modification and *in-situ* encapsulation, researchers introduced guest molecules with good luminescence properties into the MOF structure to enhance their luminescence properties [14,15]. The fluorescence sensor based on MOF has been applied in many fields [16–18].

The fluorescence emission peak of most luminescent MOFs is single peak, so it is easy to be enhanced or quenched by environmental or experimental errors in the process of analyte sensing. In addition, in the process of sensing two or more analytes with similar chemical structures and properties, it is difficult to distinguish them by single peaks. The detection of analytes by two peaks will make the fluorescence signal more stable and the sensing result more accurate [19–21]. Dye molecules achieve luminescence properties by conjugation of chromogenic and resonant group. When the dye molecules present a monodisperse state, their photoactivity is better. Even at a small concentration, the dye molecules in the solution will agglomerate [22]. Due to the influence of excitation, the energy of the agglomerated dye molecules is easily released through thermal relaxation, thus reducing the photoactivity. Therefore, we try to assemble dye with materials with regular pore structure, so as to avoid the aggregation of dye molecules, let them disperse effectively, and make them exhibit good photoactivity, such as photoluminescence and fluorescence relaxation [23,24]. Using MOF as a carrier to encapsulate dye is a meaningful means of dual-emission fluorescence sensors [25,26]. Guo *et al.* designed a RhB@MOF-5 composite material with PNPG as a substrate to detect

* Corresponding author.
E-mail address: chenxiaoli003@163.com (X.-L. Chen).

https://doi.org/10.1016/j.cclet.2023.108411
1001-8417/

β-GCU under the synergistic effect of IFE and SQE, which enriched the inspiration for achieving unique properties [27].

With the rapid growth of population and economic development, environmental problems have become increasingly prominent. In particular, industrial and agricultural pollutants cause harm to our environment and human health [28–31]. Therefore, rapid and effective detection of pollutants has become an urgent problem. As a chemical for the prevention and control of pests and diseases, pesticides play a role in regulating plant growth [32,33] and are widely used in agriculture, forestry, animal husbandry production and other fields. However, the abuse of pesticides will pollute groundwater and soil, which will not only seriously destroy the ecological environment, but also affect the sustainable development of agriculture and even directly affect human health. Therefore, in order to improve the ecological environment and health level, it is urgent to establish an efficient and sensitive method for pesticide detection. Shi *et al.* proposed a new approach to determine pesticide residue categories and concentrations in a two-stage framework, using gas sensors and using electronic nose technology to detect pesticide residue problems in soil in real time [34]. Yu *et al.* prepared a AuNPs@ CDA SERS substrate using AuNPs and biomass-based cellulose diacetate (CDA), which was able to detect pesticides and had a good linear relationship in the range of 10^{-7} g/mL to 10^{-6} g/mL, with a detection limit of 10^{-7} g/mL in water [35].

With the increasing environmental protection, the rapid detection of trace inorganic ions in water has attracted extensive attention. When the human body ingested excessive iron ions, may lead to poisoning, low immunity, easy to induce epilepsy [36,37]. Consuming excess copper ions can damage the kidneys and disrupt the gastrointestinal tract [38]. Excessive intake of aluminum ions can damage the central system and increase the risk of diseases such as Parkinson's [39,40]. Chromium ions can accumulate in the body's organs and have a long biological halflife [41,42]. At present, the rapid and sensitive detection of inorganic ions is still a challenging task. Fluorescence detection technology is widely used due to its advantages of less time, low cost, sensitive and high efficiency. Xu *et al.* synthesized a novel Mg-MOF that can detect Fe^{3+} efficiently and sensitively, as well as pesticides and antibiotics [43]. Gao *et al.* synthesized a bifunctional 3D porous MOF, it can detect Fe^{3+} in water with a detection limit of 0.09716 μmol/L. Furthermore, it has a good adsorption function for Congo red and Methyl orange dyes [44].

Ascorbate acid (AA) is an essential vitamin for humans and animal, which is found in the central nervous system and serum, plays an important role in many biochemical processes [45]. But insufficient amount of AA and a lack of will produce adverse effect to human body. Therefore, ascorbate detection has attracted extensive attention in the medical and clinical fields. Researchers have developed a number of assays for AA, but these tests still have many limitations. The detection of AA based on MOF as a fluorescence probe is simple, rapid and sensitive. As far as we know, most of the current fluorescence sensors for AA are "fluorescence off" type. So the experimenters tried to develop a fluorescence-switched MOF to detect ascorbate. Xiao *et al.* synthesized CrO_4^{2-}@Cd-MOFs, which can be used as a fluorescence switch sensor for the determination of AA with a detection limit of 7.27 ppm [46]. Guo *et al.* designed an RhB@MOF nanocomposite-based "on-off-on" probe capable of detecting Fe^{3+} and ascorbate with high selectivity [47].

To the best of our knowledge, although there are many MOFs based on 1,2,3,5-benzene tetracarboxylic acid (H_4bta), no modification of MOFs synthesized by this ligand using RhB has been reported [48–50]. Post-synthesis modification of MOF is a new method to synthesize functional MOFs, which can further optimize its physical and chemical properties and broaden its application range. Therefore, it is of great significance to study the post-synthetic modification and its properties.

In this study, RhB molecule was embedded in MOF **1**, and the composite material (RhB@**1**) was synthesized by the solvent thermal method, and the structure, composition and fluorescence characteristics were characterized. RhB@**1** was used as a fluorescence sensor to detect pesticides and metal cations. Interestingly, the composite can double detect Fe^{3+} and ascorbate by "on-off-on" fluorescence response, and the corresponding sensing detection mechanism is proposed. In addition, a logical manipulation of the necessary molecular devices was developed to monitor the changes in Fe^{3+} and AA levels in a simple way, using Fe^{3+} and AA as a chemical input signal, and the fluorescence intensity ratio (I_{415}/I_{575}) of RhB@**1** as output. It is significant that we have also successfully prepared portable test paper for FLU.

We conducted a luminescence sensing experiment for pesticides like emamectin benzoate (EMB), triadimefon (TRI), prochloraz (PRO), Pyrimethanil (PTH), 24-epibrassinolide (24-EPI), pyraclostronbin (PST), fluazinam (FLU), Zhongsheng-mycin (MYC), and imazalil (IMA). As shown in Fig. 1a, the luminescence of RhB@**1** was completely quenched in FLU, while the quenching effect of other pesticides was not good, which could indicate that the detection performance of RhB@**1** for FLU was better than that of other pesticides. Concentration titration experiment was subsequently performed to discuss the responsiveness of RhB@**1** to FLU. When the concentration of FLU increased gradually, the fluorescence intensity gradually decreased, and when added to 20 μL, the fluorescence of RhB@**1** was almost completely quenched (Fig. 1b). In addition, the Stern-Volmer (SV) equation ($I_0/I = 1 + K_{sv}[M]$) can be used to further study the relationship between FLU concentration and fluorescence intensity. In particular, a good liner relationship was observed at low concentration of FLU ($R^2 = 0.99147$), the K_{sv} value is 4.02×10^5 L/mol, but at high concentrations, deviations from linearity could be explained by self-absorption or energy transfer (Fig. 1c). Based on the slope of the fitting line and the standard deviation of the blank sample, the detection limit was calculated to be 7.94 nmol/L (at the 3σ level).

The anti-interference ability of FLU was then investigated in the presence of other pesticides. As shown in Fig. 1d, good specificity for FLU was still present in the presence of other pesticides. To delve deeper into the time dependence of RhB@**1**, we added 20 μL of FLU and measured the data at 20 s intervals. The results showed that after 20 s, the fluorescence intensity decreased significantly and remained stable, indicating that RhB@**1** is a highly sensitive sensor for FLU (Fig. S12a in Supporting information).

In order to explain the fluorescence quenching mechanism of FLU, ultraviolet spectrum experiments were carried out. The absorption spectrum of FLU overlaps effectively with the excitation peak of RhB@**1**, while the ultraviolet absorption position of other pesticides overlaps with the excitation peak of RhB@**1** can be ignored. Thus, the fluorescence quenching of FLU is mainly due to energy competition between RhB@**1** and FLU (Fig. S12b in Supporting information). In addition, the orbital energies of H_4bta and FLU calculated by density functional theory at the B3LYP/6-31+G(d) level of theory. The LUMO energy level (−0.44 eV) of FLU is lower than that of H_4bta (−0.105 eV), indicating that the fluorescence quenching may be caused by electron transfer (Fig. S12c in Supporting information). The results showed that the fluorescence quenching of FLU might be caused by energy competition and electron transfer.

First, we conducted fluorescence sensing experiments of RhB@**1** to 21 metal ions (Ag^+, Ba^{2+}, Bi^{2+}, Ca^{2+}, Cd^{2+}, Co^{2+}, Cu^{2+}, Dy^{3+}, Er^{3+}, Fe^{3+}, Eu^{3+}, K^+, La^{3+}, Mg^{2+}, Nd^{3+}, Ni^{2+}, Pb^{2+}, Pr^{3+}, Tb^{3+}, Y^{3+} and Zn^{2+}). Fig. 2a shows that RhB@**1** is almost completely quenched in Fe^{3+}, while the fluorescence intensity of other ions is enhanced or quenched to different degrees. Subsequently, the

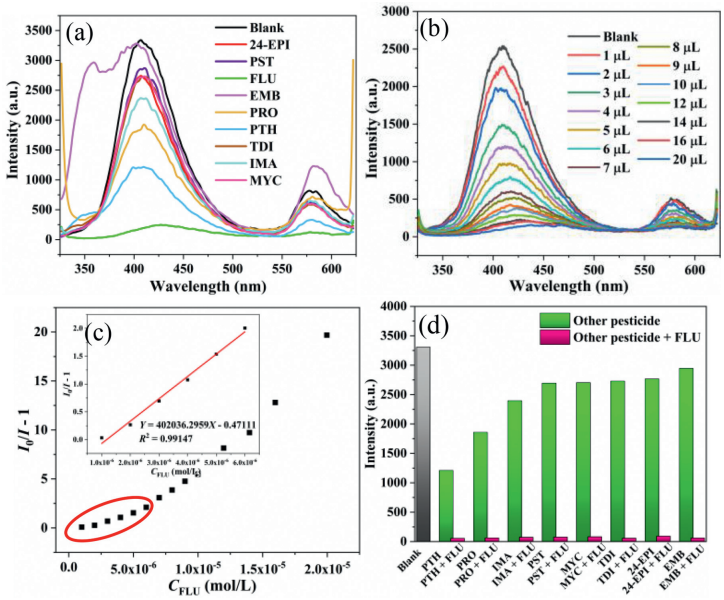

Fig. 1. (a) Fluorescence spectra of RhB@**1** with various pesticides. (b) Fluorescence spectrum of RhB@**1** in water with different concentrations of FLU. (c) Fluorescence Stern-Volmer equation and the linear relationship of I_0/I - 1 with FLU concentration. (d) Comparison of the luminescence intensity of RhB@**1** in presence of others pesticides.

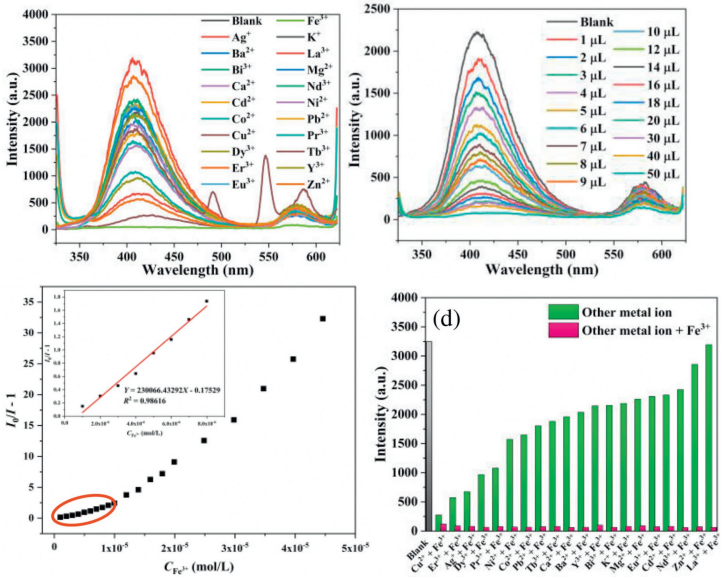

Fig. 2. (a) Fluorescence spectra of RhB@**1** with various metal ions. (b) Fluorescence spectrum of RhB@**1** in water with different concentrations of Fe^{3+}. (c) Fluorescence Stern-Volmer equation and the linear relationship of I_0/I - 1 with Fe^{3+} concentration. (d) Comparison of the luminescence intensity of RhB@**1** in presence of others metal ions.

concentration experiment was conducted to explore the recognition ability of RhB@**1** to Fe^{3+}. As shown in Fig. 2b, with the increase of Fe^{3+} concentration, the luminescence intensity of RhB@**1** gradually decreased until it was completely quenched. In addition, the Stern-Volmer (SV) equation ($I_0/I = 1 + K_{sv}[M]$) can be used to further study the relationship between Fe^{3+} concentration and fluorescence intensity. In particular, a good liner relationship was observed at low concentration of Fe^{3+} ($R^2 = 0.98616$), the K_{sv} value is 2.3×10^5 L/mol (Fig. 2c), but at high concentrations, deviations from linearity could be explained by self-absorption or energy transfer. Based on the slope of the fitting line and the standard deviation of the blank sample, the detection limit was calculated to be 7.82 nmol/L (at the 3σ level).

The anti-interference ability of Fe^{3+} was then investigated in the presence of other metal ions (Fig. 2d). Good specificity for Fe^{3+} was still present in the presence of other metal ions. In order to further study the quenching effect of anion on Fe^{3+}, 13 different anions were selected for verification. In the presence of other anions, the fluorescence quenching of Fe^{3+} was still obvious (Fig. S13a in Supporting information). Therefore, it is confirmed that RhB@**1** has high selectivity and anti-interference effect on Fe^{3+}.

To delve deeper into the time dependence of RhB@**1**, we added 50 μL of Fe^{3+} and measured the data at 20 s intervals. The results showed that after 20 s, the fluorescence intensity decreased significantly and remained stable, indicating that RhB@**1** is a highly sensitive sensor for Fe^{3+} (Fig. S13b in Supporting information).

When AA was added to the quenching system of RhB@**1** and Fe^{3+}, the quenched fluorescence was gradually recovered. Our guess is that AA reduces Fe^{3+} iron to Fe^{2+} iron. As can be seen from the equation (Fig. S14 in Supporting information), the result-

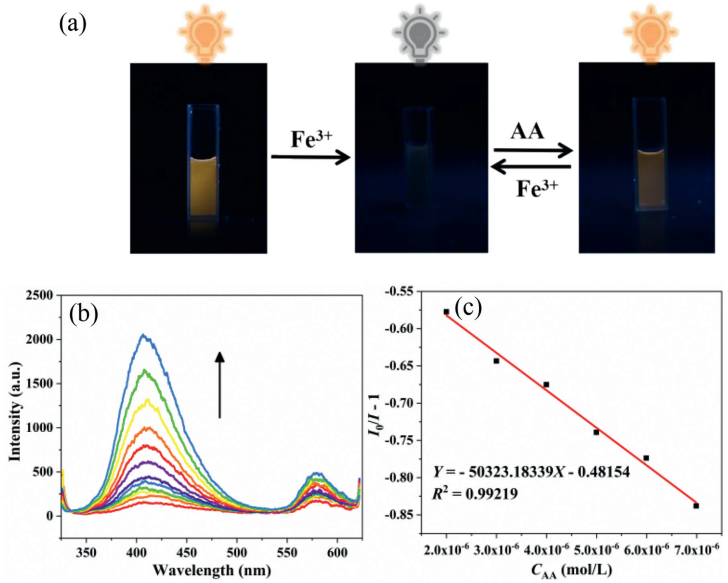

Fig. 3. (a) Corresponding photos of RhB@**1** at Fe^{3+} and AA under 365 nm UV light. (b) Fluorescence emission spectra of RhB@**1**/Fe^{3+}-system for different concentrations of AA. (c) Linear plot of AA concentration *versus* fluorescence intensity.

ing reduction product Fe^{2+} has no significant effect on the fluorescence of the system. Interestingly, the addition of Fe^{3+} quenched the fluorescence of RhB@**1**, while the addition of AA restored its fluorescence (Fig. 3a). Therefore, we designed a "Turn-on" fluorescence sensor on the system of RhB@**1** and Fe^{3+} to detect AA. First, we added AA to system RhB@**1** without Fe^{3+}, and observed the fluorescence changes of the system. Only adding AA has no effect on the fluorescence of the system (Fig. S15 in Supporting information). So it is verified that the redox reaction between Fe^{3+} and AA in the system restores the fluorescence. We also studied the effect of time on fluorescence recovery, and it can be seen that after 40 min, fluorescence intensity was basically stable and fluorescence was basically recovered (Fig. S16 in Supporting information). Then we found that in the system of RhB@**1** and Fe^{3+}, the fluorescence intensity gradually increased and the fluorescence gradually recovered by increasing the concentration of AA (Fig. 3b). The concentration of AA is linearly related to the fluorescence intensity at low concentration (Fig. 3c), and the detection limit of AA is calculated to be 0.06 μmol/L, which is lower than the concentration of AA in biological samples. It has potential application value in practical life. In addition, we also compared MOF or composite material sensors reported in other literatures to detect Fe^{3+} and AA, and found that our developed RhB@**1** was superior to other sensors (Table S2 in Supporting information).

In order to further explore the quenching mechanism of Fe^{3+} ions, we firstly confirmed by XRD that the skeleton structure of the sample did not collapse before and after Fe^{3+} ion detection (Fig. S17 in Supporting information). After a cycle, it was found that RhB@**1** still maintained a good morphology after adding Fe^{3+} and AA, indicating its considerable stability (Fig. S18 in Supporting information). The absorption spectra of Fe^{3+} and the fluorescence spectra of RhB@**1** effectively overlap, resulting in an IFE mechanism between RhB@**1** and Fe^{3+} (Fig. 4a). The band gap of RhB@**1** is 2.96 eV (Fig. 4b). Fig. 4c shows the VB-XPS results, which indicate that the valence band maximum of RhB@**1** is 1.79 V. Using the empirical, $E_{VB} = E_{CB} + E_g$, the conduction band minimum of RhB@**1** is −1.17 V. Since the electrode potential of Fe^{3+}/Fe^{2+} is 0.77 V, it is between the range of CB and VB of RhB@**1**. Therefore, when RhB@**1** is irradiated by light, the electrons in the valence band (VB) are excited to the conduction band (CB) and then transferred to the d orbital of Fe, which quenches the fluorescence

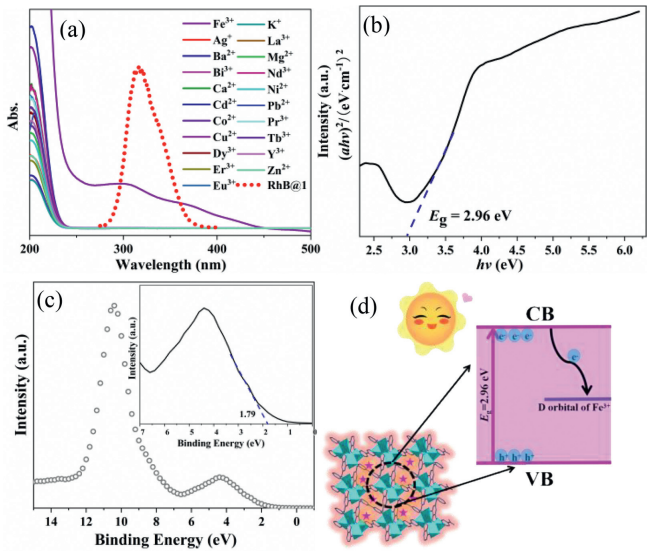

Fig. 4. (a) The excitation spectra of RhB@**1** and UV-vis absorption of Fe^{3+} and other metal ions in aqueous solution. (b) Corresponding Tauc plots of the RhB@**1**, and the dotted line is the linear fitting. (c) VB-XPS spectra of RhB@**1**. (d) Principle scheme of PET mechanism between Fe^{3+} and RhB@**1** composites.

of RhB@**1** by the PET mechanism (Fig. 4d). Fluorescence attenuation experiments showed that the fluorescence lifetime remained unchanged after adding Fe^{3+}, indicating that the quenching mechanism may also follow the static quenching effect (SQE) (Fig. S19 in Supporting information). We speculated that the possible mechanisms leading to fluorescence quenching are that firstly, energy transfer from MOF to the analyte reduces the fluorescence emission intensity of RhB@**1** at 415 nm, and secondly, in the presence of Flu/Fe^{3+}, energy transfer from MOF to Flu/Fe^{3+} inhibits or blocks energy transfer from MOF to RhB, thus quenching the fluorescence emission peak at RhB@**1** at 575 nm (Fig. S20 in Supporting information) [51].

In summary, a unique fluorescence dual emission sensor was successfully fabricated by *in situ* synthesis. It can not only observe the change of luminescence color through the naked eye,

but also be well quenched by quench FLU and Fe^{3+} with low detection limits. It is worth mentioning that after quenching Fe^{3+} and adding AA, the fluorescence of the sensor gradually recovered, forming a rare "on-off-on" sensor. In addition, RhB@**1** as a novel logic gate device, enriches the component modules of the logic gate switchgear and provides a prospect for the practical application of dye@MOF luminescent composites in biochemical detection. Interestingly, a visual portable test paper with good selectivity and high sensitivity was developed, which can be used for rapid detection of FLU, showing its broad application prospect.

Declaration of competing interest

The authors declare that they have no known competing financial interests or personal relationships that could have appeared to influence the work reported in this paper.

Acknowledgments

This work was supported by National Natural Science Foundation of China (No. 21763028), Science and Technology project of Shaanxi Province (Nos. 2022NY-071, 2022QFY07-05, 2022JZ-49).

Supplementary materials

Supplementary material associated with this article can be found, in the online version, at doi:10.1016/j.cclet.2023.108411.

References

[1] T. Skorjanc, D. Shetty, M. Valant, ACS Sens. 6 (2021) 1461–1481.
[2] Y. Wang, H. Li, X. He, Z. Xu, Inorg. Chem. 60 (2021) 15001–15009.
[3] H. Li, M. Eddaoudi, M. O'Keeffe, O.M. Yaghi, Nature 402 (1999) 276–279.
[4] H. Chai, G. Zhang, C. Jiao, Y. Ren, L. Gao, ACS Omega 5 (2020) 33039–33046.
[5] X.L. Chen, L. Shang, L. Liu, et al., Dyes Pigments 196 (2021) 109809–109821.
[6] L. Shang, X.L. Chen, L. Liu, et al., J. Solid State Chem. 304 (2021) 122575–122588.
[7] Z.D. Zhou, Z.L. Xu, D. Wang, et al., Chin. J. Struct. Chem. 41 (2022) 2209087–2209093.
[8] X.M. Tian, S.L. Yao, C.Q. Qiu, et al., Inorg. Chem. 59 (2020) 2803–2810.
[9] H. Zhao, Q. Xia, H. Xing, D. Chen, H. Wang, ACS Sustain, Chem. Eng. 5 (2017) 4449–4456.
[10] A. Sarkar, A. Adhikary, A. Mandal, T. Chakraborty, D. Das, Cryst. Growth Des. 20 (2020) 7833–7839.
[11] S. Chang, C. Liu, Y. Sun, et al., ACS Appl. Nano Mater. 3 (2020) 2302–2309.
[12] N. Bhardwaj, S.K. Bhardwaj, J. Mehta, et al., ACS Appl. Mater. Interfaces 9 (2017) 33589–33598.
[13] Y. Shu, Q. Ye, T. Dai, Q. Xu, X. Hu, ACS Sens. 6 (2021) 641–658.
[14] Y. Li, B.L. Chai, H. Xu, et al., Inorg. Chem. Front. 9 (2022) 1504–1513.
[15] Y. Zhang, M. Sun, M. Peng, et al., Chin. Chem. Lett. 34 (2023) 107478.
[16] N. Sun, B. Yan, Sens. Actuators B: Chem. 261 (2018) 153–160.
[17] W. Meng, Y. Wen, L. Dai, et al., Sens. Actuators B: Chem. 260 (2018) 852–860.
[18] Z. Wei, D. Chen, Z. Guo, et al., Inorg. Chem. 59 (2020) 5386–5393.
[19] B. Shi, X. Zhang, W. Li, et al., Food Chem. 400 (2023) 133995–134005.
[20] J. Li, Y. Dai, J. Cui, et al., Talanta 251 (2023) 123817–123827.
[21] K. Xing, R. Fan, X. Du, et al., Sens. Actuators B: Chem. 228 (2019) 307–315.
[22] X.J. Lei, X.Y. Hou, S.N. Li, et al., Inorg. Chem. 57 (2018) 14280–14289.
[23] J. Hassanzadeh, H.A.J. AlLawati, I. AlLawati, Anal. Chem. 91 (2019) 10631–10639.
[24] X. Xu, X. Lian, J. Hao, C. Zhang, B. Yan, Adv. Mater. 29 (2017) 1702298–1702305.
[25] D.M. Chen, N.N. Zhang, C.S. Liu, M. Du, ACS Appl. Mater. Interfaces 9 (2017) 24671–24677.
[26] Y. Zhang, L. Gao, S. Ma, T. Hu, Cryst. Growth Des. 22 (2022) 2662–2669.
[27] L. Guo, Y. Liu, R. Kong, et al., Sens. Actuators B: Chem. 295 (2019) 1–6.
[28] H. Eskandari, M. Amirzehni, J. Hassanzadeh, B. Vahid, Microchim. Acta 287 (2020) 673–683.
[29] H. Ding, C. Li, H. Zhang, et al., Chin. Chem. Lett. 34 (2023) 107725.
[30] T. Wang, C. Zhao, L. Meng, et al., Chem. Eng. J. 451 (2023) 138624–138632.
[31] K. Wang, T.F. Zheng, J.L. Chen, et al., Inorg. Chem. 61 (2022) 16177–16184.
[32] R.M. Abdelhameed, M. El-Naggar, M. Taha, et al., J. Mol. Struct. 1199 (2020) 127000–127009.
[33] D.K. Singha, P. Majee, S. Mandal, S.K. Mondal, P. Mahata, Inorg. Chem. 57 (2018) 12155–12165.
[34] X.H. Shi, Y.H. Qiao, X.Y. Luan, et al., Chin. J. Anal. Chem. 50 (2022) 100124–100133.
[35] D.Guo H.Yu, H. Zhang, et al., Spectrochim. Acta A 285 (2023) 121930–121938.
[36] T. Zhou, S. Liu, X. Guo, et al., Cryst. Growth Des. 21 (2021) 5108–5115.
[37] D.G. Cai, C.Q. Qiu, Z.H. Zhu, et al., Inorg. Chem. 61 (2022) 14770–14777.
[38] S. Senthilkumar, R. Goswami, V.J. Smith, et al., ACS Sustain. Chem. Eng. 6 (2018) 10295–10306.
[39] X. Zheng, Y. Zhao, P. Jia, et al., Inorg. Chem. 59 (2020) 18205–18213.
[40] L.H. Wu, S.L. Yao, H. Xu, Chin. Chem. Lett. 33 (2022) 541–546.
[41] X.Y. Xu, B. Yan, Sens. Actuators B: Chem. 222 (2016) 347–353.
[42] A. Mandal, A. Adhikary, A. Sarkar, D. Das, Inorg. Chem. 59 (2020) 17758–17765.
[43] N. Xu, Q. Zhang, B. Hou, Q. Cheng, G. Zhang, Inorg. Chem. 57 (2018) 13330–13340.
[44] L.L. Gao, T. Gao, Y. Zhang, T. Hu, Dyes Pigments 197 (2022) 109945–109954.
[45] C. Guo, Q. Jin, Y. Wang, et al., Sens. Actuators B: Chem. 234 (2016) 184–191.
[46] J. Xiao, J. Liu, M. Liu, G. Ji, Z. Liu, Inorg. Chem. 58 (2019) 6167–6174.
[47] L. Guo, Y. Liu, R. Kong, et al., Anal. Chem. 91 (2019) 12453–12460.
[48] C. Wei, C.K. Xia, Y.L. Wu, et al., Polyhedron 89 (2015) 189–195.
[49] C.K. Xia, Y.Y. Min, K. Yang, et al., Cryst. Growth Des. 18 (2018) 1978–1986.
[50] C.K. Xia, F. Wu, K. Yang, et al., Polyhedron 117 (2016) 637–643.
[51] J.W. Zhang, H.T. Zhang, Z.Y. Du, et al., Chem. Commun. 50 (2014) 1092–1094.